Designing Agent-based Simulation to Assess the Impact of Coordination Schemes on Infrastructure Networks Resilience

A thesis submitted in partial fulfillment of the requirements for the degree of
Master of Science at George Mason University

By

Mark Herman Dsouza
Bachelor of Science
Mumbai University, 2019

Director: Dr. Shima Mohebbi, Professor
Department of Computer Science

Fall Semester 2022
George Mason University
Fairfax, VA

Dedication

I dedicate this thesis to my family especially my Mom and Dad who have made it possible. Without their support and motivation it would not have been possible.

Acknowledgments

I am grateful to my advisor, Dr. Shima Mohebbi, for her incredible support, encouragement, and countless opportunities that she provided me. I would also like to thank my committee members for their time, knowledge, and guidence that they provided along the way. Additionally, I would like to thank PhD student Babak Aslani for his encouragement, guidance, and instruction throughout my Master's research. Lastly, this work was partially supported by the National Science Foundation under Grant Number 1638301. Any opinions, findings, and conclusions or recommendations expressed in this material are those of the author and do not necessarily reflect the views of the National Science Foundation.

Table of Contents

Page

List of Tables . . . vi

List of Figures . . . vii

Abstract . . . ix

1 Introduction . . . 1

2 Literature Review . . . 4

2.1 Agent-based Modelling . . . 4

2.2 Collaboration Schemes . . . 5

3 Model Development . . . 7

3.1 Graph Representation of Infrastructure Networks . . . 7

3.2 Population of Agents . . . 7

3.3 Collaboration Schemes . . . 14

4 Implementation and Results . . . 18

4.1 Parameters and Verification . . . 19

4.2 Computational Study . . . 21

4.2.1 Performance Metrics . . . 22

4.2.2 Simulation Output . . . 25

5 Conclusions . . . 40

Bibliography . . . 42

List of Tables

Table Page

4.1 Road traffic verification result 21

4.2 Disruptive scenarios 22

4.3 Area under the curve for different Communication Protocols 39

List of Figures

Figure Page

3.1 Statechart for maintenance crew agents 9

3.2 Statechart for traffic light agent 10

3.3 Statechart for pipe and road agent 11

3.4 Unified Modeling Language class diagram of the multi-agent simulation model 13

4.1 Simplified interdependent water and transportation network 18

4.2 Network resilience curves for physical failure scenarios and no communication protocol . 26

4.3 Network resilience curves for cyber-physical failure scenarios and no communication protocol 27

4.4 Network resilience curves for physical failure scenarios and leader-follower coordination protocol 28

4.5 Network resilience curves for cyber-physical failure scenarios and leader-follower coordination protocol 29

4.6 Network resilience curves for physical failure scenarios and decentralized coalition formation protocol 30

4.7 Network resilience curves for cyber-physical failure scenarios and decentralized coalition formation protocol 31

4.8 Ranked Ordered resilience curve for physical failures scenarios and no communication protocol 33

4.9 Ranked Ordered resilience curve for cyber-physical failure scenarios and no communication protocol 34

4.10 Ranked Ordered resilience curves for physical failures and leader-follower coordination protocol 35

4.11 Ranked Ordered resilience curves for cyber-physical failure scenarios and leader-follower coordination protocol 36

4.12 Ranked Ordered resilience curves for physical failure scenarios and decentralized coalition formation protocol 37

4.13 Ranked Ordered resilience curves for cyber-physical failure scenarios and decentralized coalition formation protocol 38

Abstract

DESIGNING AGENT-BASED SIMULATION TO ASSESS THE IMPACT OF COORDINATION SCHEMES ON INFRASTRUCTURE NETWORKS RESILIENCE

Mark Herman Dsouza

George Mason University, 2022

Thesis Director: Dr. Shima Mohebbi

Critical infrastructures systems are governed by several sectors working together to maintain social, economic, and environmental well-being. Their cyber-physical interdependencies, on the other hand, influence their performance and resilience to routine failures and extreme events. To balance investment and restoration decisions before, during, and after disruptive events, different mathematical formulations and solutions, mainly focused on centralized view, were presented in the literature. While necessary and useful, not all physical and dynamic characteristics of infrastructure systems and their decision makers can be modeled via mathematical models. In this study, we take a different approach and utilize agent-based modeling to simulate city-scale interdependent infrastructure networks as a complex adaptive system. We first model each infrastructure as a weighted graph with relevant geospatial attributes. Decision makers (e.g., maintenance crew) for each infrastructure sector are represented by intelligent agents.

We then define three information and coordination structures among agents, including no communication, leader-follower, and decentralized coalitions. The framework is applied to the interdependent water distribution and road networks in the City of Tampa, FL. We simulate different magnitudes of cyber-physical failures, evaluate resource allocation decisions, made by agents under each coordination structure, and quantify the aggregated resilience. Specifically, we develop a rank aggregation performance measure to evaluate restoration effectiveness for each scenario. This research helps municipalities to quantify the impact of their collective decision making and identify the best coordination structures when interdependencies are modeled in infrastructure systems.

Chapter 1: Introduction

Modern world heavily relies on infrastructure systems. Critical infrastructures provide critical services such as energy and water; and connects communities via transport and communications networks, enabling the flow of goods and information. Infrastructure systems based on energy, transport, telecommunications are highly interdependent. Such systems with cyber-physical interdependencies are vulnerable to random failures, due to aging infrastructures, and natural hazards [1]. It is, therefore, essential for infrastructures to be prepared for the threats that can be anticipated and to be able to respond to the threats, so that it continues to provide the necessary services on which modern world depends.

Infrastructure resilience is the ability to withstand, adapt to changing conditions, and recover positively from shocks and stresses [2]. Resilience enhancement in infrastructures requires assessing the capacity of sub-systems to respond to disturbances and how different infrastructures connect and support each other's functionality. Hurricane Sandy, for instance, motivated the federal government to examine ways to improve community and infrastructure resilience so that communities are better prepared for existing and future threats and to ensure that federal agencies incorporate key principles of resilience into their formulation and evaluation [3]. Collaboration is a form of collective action and governance that brings together organizations to work across organizational boundaries to solve problems that cannot be effectively addressed by any organization separately [3]. Sandy Regional Infrastructure Resilience Coordination (SRIRC) Group identified areas for improvement and potential challenges, provided briefings on overlapping program efforts, served as a source of knowledge and encouraged inter-agency collaboration. The massive coordination and data tracking efforts, led by SRIRC, were the impetus for developing a collaborative geographic tool [4]. It displays the physical location of all ongoing recovery projects for a given disaster alongside a collaborative online platform, known as MAX-TRAX. MAX-TRAX is now used in disaster recovery missions across the country by Federal Emergency Management Agency (FEMA) and its partners from states, tribes, territories, local governments and inter agency partners [4].

Another research studied the causes of tremendous infrastructure failures and disruptions during hurricane Harvey in the city of Houston and Harris County [5]. They used a combination of surveys, field visits, and network analysis to assess the relationships and interdependencies between key stakeholders and decision-makers, existing infrastructure and resilience plans, and the physical infrastructure itself. Their study found that collaboration between stakeholders (policymakers and decision-makers across sectors, state and local government and non-governmental organizations) was fragmented, with isolation that negatively affect resilience and hazard mitigation planning. Also, the dependencies of one infrastructure system on another are not fully accounted in their study. The coordination among infrastructure sectors, while necessary, faces a number of challenges. One of the key challenges is the lack of availability of appropriate information at the correct time which negatively affects the collaboration process [3]. In addition, given the heterogeneous nature of infrastructures, various resource allocation schemes are usually performed, leading to sub-optimal utilization of available resources that may even cause further cascading failure [6].

Majority of existing works in the literature have focused on developing mathematical models in different forms including linear Mixed Integer Programming (MIP), Non-linear MIP, bi-level MIP, and tri-level MIP to study infrastructure systems after a disruptive event. The mathematical frameworks assume that infrastructure systems operate in a centralized decision-making environment and simplify the evolving dynamics of networks in response to changes over time [7]. In addition, optimization models become computationally intractable if all physical and dynamic characteristics of infrastructure systems and their decision makers are captured (e.g., see [8]). As a result, there is an emergent need to develop novel frameworks to capture and model the dynamic processes and interactions between the complex infrastructure systems [9]. Simulations methods such as agent-based models (ABMs) provide a dynamic framework to explore, analyze, and understand the impacts of individual actors' behavior and their interactions with cyber-physical infrastructure systems [10]. ABMs are capable of capturing and generating a comprehensive range of nonlinear behavior compared to mathematical models, providing a unique opportunity for policy-makers to evaluate different policy scenarios, explore their consequences, and extract practical insights [11].

Therefore, in this study, we focus on agent-based models to simulate simplified city-scale interdependent infrastructure systems. We aim to develop a scalable framework populated with different types of agents to incorporate the key players in the decision-making process of infrastructure systems. Geospatial databases are exploited to design and embed algorithms for routing and minimum cost flow/shortest path, and to detect co-location interdependency among physical components of interdependent water and road networks. We include a network structure analysis module to quantify the accessibility of transportation network and address the island scenario challenge arising in the post-disaster recovery of a disrupted network. We then define three collaboration structures among agents, no communication, leader-follower, and decentralized coalitions, for resource allocation to assess the impact of each structure. We use AnyLogic, a Java-based platform, to implement the simulator engine and simulate different magnitudes of cyber-physical failures to quantify the aggregated resilience under each coordination structure. In addition to total network resilience index, we develop a rank-based performance measure to evaluate the recovery efficiency in the interdependent networks.

Following this section, the remainder of this thesis is organized as follows: In Section 2, he relevant literature and gaps are presented. Section 3 is devoted to a detailed explanation of the model development. Section 4 provides implementation steps, verification, and the computational results for the case study in the City of Tampa, FL. Finally, Section 5 will provide concluding remarks, limitations, and the future research directions.

Chapter 2: Literature Review

The two key components of this study are agent-based simulation and the collaboration structure among agents. This modeling approach has been applied to interdependent critical infrastructures in prior research, although the assumptions and applications vary between prior research and this study.

2.1 Agent-based Modelling

Agent-based modeling has become a popular methodology in the literature of resilience assessment. It can capture the dynamic behaviors of decision-makers, resource allocations, and different types of interdependencies among interdependent infrastructure networks. Among others,[12] developed critical infrastructure simulation which uses a hybrid approach on the basis of the mostly qualitative information drawn from infrastructures stakeholders to set up a fault propagation simulation. In their model, dynamics of each agent is described via Fuzzy logic quantities to consider the uncertainties that characterize the knowledge about these infrastructures.

[13] attempted to represent cascading failure propagation within a multi-infrastructure system and identified robust investment strategies to enhance infrastructure resilience. They investigated empirical approaches, agent-based approaches, system dynamics approaches and network-based approaches. [14] built a neural model consisting of multiple agents and the communication between them is learned alongside their policy. They demonstrated the ability of the agents to learn to communicate amongst themselves, yielding improved performance over non-communicative agents and baselines. [15] focused on the behavior of complex systems after they experience disruptive events that impact their performance. Agent-based simulation with an adaptive algorithm was used to assess the effectiveness of strategies that system owners employ to restore the system. [16] developed a leader–follower agent-based model to interpret local social

interactions and collective behavior. In their model, a pedestrian agent can establish informal and transient leader–follower relationships with others while adjusting its behavioral patterns as required by the situation.

[17] used multi-agent based deep reinforcement learning to model the critical infrastructure interdependencies and see the propagation of cascading failure in real-time during a flooding event. They concluded that visualizing the resultant progress in a spatiotemporal environment will help in easy visualization and better decision-making during emergency situations. In a recent study, [9] adopted an ABM framework to simulate and comprehend the underlying mechanisms such as forewarning duration and social network types affecting the resilience of infrastructure system. The results showed that restoration prioritization strategy and equitable resilience could be improved by focusing on vulnerable populations during extreme events.

The majority of previous works, using ABM frameworks, simulated physical failures in small or medium scale networks. This leaves a gap for scalable simulation-based framework evaluating the impact of compounded cyber-physical threats and their propagation on the resilience of infrastructure networks.

2.2 Collaboration Schemes

Focusing on collaboration schemes among agents in a decentralized environment, information structures have been shown to be crucial in the progress of understanding dynamic interactions and teams [18]. The designer of a system may impose such structures, or the agents may have agreed upon it in a particular communicative interaction endriss2003logic.

[19] provided a tutorial paper with a comprehensive characterization of information structures. Information structures are classified as (1) classical, (2) partially nested (alternatively also called overlapping), and (3) non-classical. In classical information structures, all agents receive the same information and have perfect recall. If there is only one team member, then such information structures are called strictly classical resulting in team decision problems that are typical centralized stochastic control problems. In partially nested information structures, there are some agents who have a nonempty intersection of their information structures while they have perfect recall. Any information structure that is not classical, or partially nested,

is called non-classical and can be further classified as the n-step delayed-sharing (see [20]), periodic sharing, or no sharing information, where the agents do not share any information. Among others, [21] proposed a framework to deal with delays. Their proposed delay-aware multi-agent reinforcement learning algorithm helped reduce the performance degradation introduced by delay.

Having focused on possible coalition formations by agents, [22] studied agents in dynamic and uncertain environments such that agents' tasks evolve during execution and resource availability may vary rapidly and be unpredictable. They used parallel and non-return broadcast, based on decentralized multilateral negotiation, to form auto-stabilizing coalitions. They demonstrated that the proposed approach was able to handle the uncertainty of agents such as dependencies, preferences and availability, and to reach stability. In another study, [23] tried to find a feasible coalition structure. They proposed a decentralized based approach of token passing between agents, which is divided into various rounds. The proposed approach has two stages which gradually tries to improve the coalition structure. They used constraint satisfaction problem techniques to solve large-scale instances. They did not apply the proposed model to any real-world problem. The results also showed that centralized approach provided optimum results compared to decentralized. [24] proposed a model which uses the reputation of individuals connected by a network, rather than using reward analysis for every possible coalition. In their model, the strength of social ties determines the preferred partnerships for cooperative work. [25] tried to find the contribution that each agent makes to a coalition. They used Shapley value to assess the average contribution of each agent to all possible coalition.

The review of the literature reveals that cooperative management strategies can enhance the resilience of infrastructure systems facing disruptive events (e.g., [26]). However, to the best of our knowledge, there is no comprehensive quantitative modeling of coordination structures on the improvement of infrastructure networks resilience. Therefore, in this thesis, we study the impact of collaboration structures among decision-makers. Specifically, we focus on: (a) no communication, (b) leader-follower (water sector is the leader and transportation sector is the follower), and (c) coalitional structures. We will simulation different magnitudes of compound cyber-physical failures and compare resource allocation strategies with respect to collaboration structures.

Chapter 3: Model Development

3.1 Graph Representation of Infrastructure Networks

We define the transportation and water distribution infrastructures as networks for the proposed agent-based modelling framework.

The water distribution network can be presented as a directed graph $\mathcal{W} = (\mathcal{V}^w, \mathcal{E}^w)$, where $\mathcal{V}^w \in \{V_1^w, V_2^w, ..., V_{N1}^w\}$ characterize the set of nodes across the network (e.g., pump stations, valves, reservoirs, and household demand points) and $\mathcal{E}^w \in \{E_1^w, E_2^w, ..., E_{M1}^w\}$ represent the edges (e.g., pipe) in the network. $N1$ and $M1$ denote the number of nodes and edges in the network, respectively. Each $E_{ij}^w \in \mathcal{E}^w$ is a directed link from node V_i^w to node V_j^w with a flow such as f_{ij}. Following a disruptive event, the failed components (pipes) of the water network are defined as $\bar{F}^w$ and the unaffected pipes are F^w such as $\bar{F}^w \cup F^w \equiv \mathcal{E}^w$.

Similarly, the transportation network can be represented as a directed graph $\mathcal{T} = (\mathcal{V}^t, \mathcal{E}^t)$, where $\mathcal{V}^t \in \{V_1^t, V_2^t, ..., V_{N2}^t\}$ characterize the set of nodes (e.g., road intersection) and $\mathcal{E}^t \in \{E_1^t, E_2^t, ..., E_{M2}^t\}$ represent the edges (e.g., roads) in the network. $N2$ and $M2$ denotes the number of nodes and edges in the network, respectively. Each $E_{ij}^t \in \mathcal{E}^t$ reflects that intersections V_i^t and V_j^t are linked to each other through a road, enabling traffic movement t_{ij} between two points. Similar to the water network, we denote the disrupted roads by $\bar{F}^t$ and the operational road segments by F^t such as $\bar{F}^t \cup F^t \equiv \mathcal{E}^t$.

3.2 Population of Agents

We characterize each population of agents by the associated states, set of actions, the decision rules managing the behavior of agents, and the main processes attributed to each type of the agents in the developed model.

Car agent

The car agents are denoted by $c \in \mathcal{C}$, which start moving from a random origin intersection such as $\mathcal{V}_O^t \in V^t$ to a destination $\mathcal{V}_D^t \in V^t$. As there are multiple paths to reach from $\mathcal{V}_O^t$ to $\mathcal{V}_D^t$, we implemented the Dijkstra shortest path algorithm. The algorithm finds the shortest distance (or interchangeably path) from a starting node to the target node in a weighted graph. Algorithm 1 shows the dynamic routing algorithm we adopted in the proposed framework to guide each car. Each agent c starts moving with 60 km/h speed, and is able to accelerate by 1.8 m/sec^2. While we set the preferred speed during the movement to 60 km/h, we adjusted the maximum deceleration to 4.8 m/sec^2.

Algorithm 1: Dynamic Routing of Cars based on Origin-Destination pairs

$\mathcal{T} = (\mathcal{V}^t, \mathcal{E}^t)$

Randomly Generate $\mathcal{C}$ based on the average daily traffic flow

for all $c \in \mathcal{C}$ **do**

  $\mathcal{O}$= Origin $\mathcal{V}^t$ from a random zone;

  $\mathcal{D}$ = Destination $\mathcal{V}^t$ from a different zone;

  $\mathcal{P}$ = The shortest path using Dijkstra Shortest Path Algorithm on $\mathcal{T}$;

  Move c to commute from $\mathcal{O}$ to $\mathcal{D}$ following path $\mathcal{P}$;

end for

Maintenance Crew Agent

The maintenance agents (hereafter denoted by $m \in \mathcal{M}$) are responsible for the restoration of disrupted pipes and roads in the water and transportation networks. We assign a skillset attribute to each agent as $0 \le \alpha_m \le 1$. If this coefficient is equal to 1, it reflects that the agent is experienced and there is no difference between the expected and actual restoration time for each failed component. Because different decision-makers govern the infrastructure systems, we separate the maintenance crew agents for water, transportation, and traffic lights such that $m^w \cup m^t \cup m^l \equiv \mathcal{M}$. Consistent with the previous notations, $m^w \in \mathcal{M}$ are the maintenance crew agents for the water distribution network, and $m^t \in \mathcal{M}$ are the agents associated with the transportation infrastructure. Similarly, we assign a population of maintenance crew denoted as $m^l \in \mathcal{M}$ to restore the disrupted cyber components (i.e., traffic lights).

As depicted in Fig. 3.1, each m agent can be in four separate states. The agent is in state *idle* if it is not moving toward any disrupted component or moving back from a restorative action to the base position (home). Following receiving a message for restoring a pipe or road, the agent transitions to *goToFix* state, indicating that the agent is assigned to a component. Upon arriving at the disrupted component and initiating the restoration activity, the agent moves to the *fixing* state, which is the actual repair time. Finally, having finished the restoration, the agent goes to *goBackHome* state, indicating that the maintenance crew is going back to the designated initial physical point. After arrival, the agent circles back to the *idle* state.

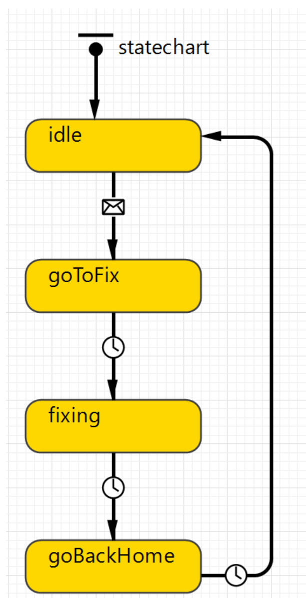

Figure 3.1 Statechart for maintenance crew agents

The restoration process of the maintenance crew starts by forming a failed component queue for both infrastructures. Following that, the restoration in both networks begins by assigning the nearest agent m

(identified by the Dijkstra shortest path algorithm) to the disrupted component. Once the agent is assigned, it is transferred to the destination pipe or road. The agent m requires to spend the calculated restoration time for the failed element. Then, the agent is sent back to the original position and the states changes to *idle*, making them available for the next possible restoration assignment. This iterative process continues until the initial failure list for water and transportation is empty.

Traffic Lights Agent

Traffic light agents (hereafter denoted by $l \in \mathcal{L}$) represent the cyber component, embedded in the infrastructure systems. Each agent l is positioned in the intersection across the transportation network, controlling the movement of cars along the roads. The traffic light agent goes through three states: Green, yellow, and red. Fig. 3.2 shows that the transition between each state (or interchangeably light) happens after a certain time (phase).

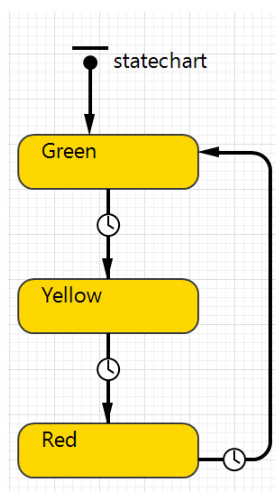

Figure 3.2 Statechart for traffic light agent

Pipe Agent

The pipe agents defined as $p \in \mathcal{P}$ represent the physical components in the water network graph such that $\mathcal{P} \subset \mathcal{W}$. The pipe agent p can be in two states: *working* and *blocked* (see Fig. 3.3). The agent is in the *working* state when it is operational, and a flow is passing through from a supply node (e.g., a tank or reservoir) to a demand node (e.g., a household point). However, following a disruptive event, the agent can transition to *blocked* state if it is affected by the event and is not able to operate normally.

Road Agent

The road agent is defined as $r \in \mathcal{R}$ representing the physical components (roads and intersections) in the transportation infrastructure graph such that $\mathcal{R} \subset \mathcal{T}$. Similar to the pipe agent, the road agent r can also be in two states including *working* and *blocked* (see Fig. 3.3). The agent is in the *working* state when the road is operational, and the cars can travel through the road segments. However, following a disruptive event, the road agent r can transition to *blocked* state if the road is blocked and is not accessible anymore.

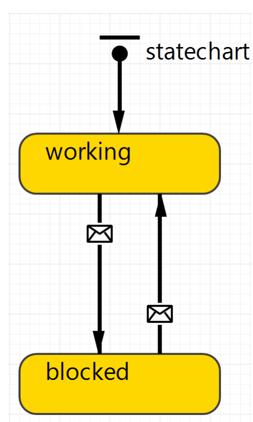

Figure 3.3 Statechart for pipe and road agent

Agents Interaction Within the Simulation Environment

Emergent behavior in an ABM model results from the interactions of individual agents. There are various types of interactions among defined agents in the proposed simulation framework. For example, the car agents interact with the road agents directly. In other words, when one road segment is in the *disrupted* state, the cars cannot pass through that segment. Moreover, the car agent also interacts with the traffic light agents when being in *yellow* and *red* states which force the moving car agents to slow down and ultimately stop. The road and pipe agents also interact to capture the interdependency among physical networks when the failure of one pipe agent also enforces the interconnected road agent to move to the *disrupted* state (see Algorithm 2). The maintenance crew agents (separated for each network and traffic lights) exchange information with the pipe, road, and traffic light agents. Specifically, when one component is failed due to a disruptive event, the new state informs the associated maintenance crew agents to update the repair list and restore the component depending on the availability of resources. Finally, the traffic light agents also impact the movement of maintenance crew agents when traveling from their station/base to the restoration area. The interactions among agents within the developed simulation framework are visualized using a class diagram in Fig. 3.4.

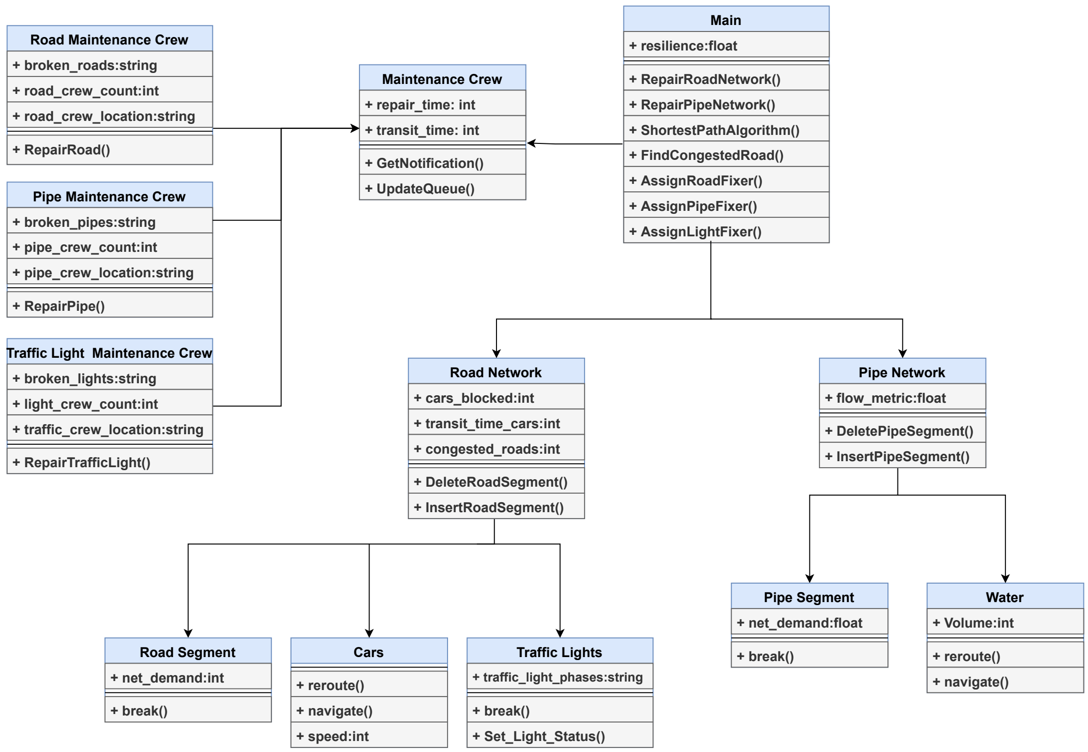

Figure 3.4 Unified Modeling Language class diagram of the multi-agent simulation model

---

Algorithm 2: Cascading Failure

Input: Roads = roads collection, Pipes = pipe collection.

while *no RoadBlocked is True* **do**

Select random road from Roads;

Block the road; isRoadBlocked is True

Delay the cars in blocked road until the road is fixed; areRoadBloked is True

Check connected links;

if isRoadBlocked is False for any connected link **then**

Distribute the cars to the random available roads;

Delay the cars before entering the blocked road until a road becomes available;

end if

end while

while *no PipeBlocked is True* **do**

Select random pipe from Pipes;

Close the pipe;

if isPipeConnected with roads is True **then**

Block the road and go to 6;

Block the pipe;

Block the pipe;

end if

Calculate the Performance indicators;

end while

3.3 Collaboration Schemes

No Communication Protocol

In this protocol, groups of agents are present in the environment, both of which independently make a decision given the receiving information and pre-defined decision rules. We assume that the maintenance crew for road and water departments are separate entities with no information sharing between them. The information received by each group of maintenance crew is limited to their own group. Each group receives a different task set which consists of failed components related to their network. The sets are updated based on the information received from the environment. No communication protocol can work well if there are no interdependent components in the networks. As a result, we expect to observe redundant resource allocation decisions.

Leader-Follower Coordination Protocol

This protocol reflects the situation where a group of agents with external inputs are selected as *leaders* to guide a group of agents as *followers* such that the entire system can achieve consensus with respect to certain performance criteria. In our simulation model, we assume the water maintenance crew act as the leader and update the information to the follower, i.e., road maintenance crew. In specific, the leader updates the information to the follower agent for interdependent components. After restoring a pipe which is co-located with a road, the leader agent (water maintenance crew) updates the set of failed components for the follower by adding the co-located road to their list of failed components. This protocol is expected to avoid redundant decisions made in the no communication setting and improve the efficiency of restoration process.

Decentralized Coalition Formation Protocol

In this collaboration structure, we present a decentralized coalition formation(DCF) and task allocation mechanism. In this protocol, the coalition formation and task allocation mechanism is fully decentralized. Initially, agents only know their own characteristics, the global task, interdependency and their respective requirements, and the set of the available agents. Gradually, agents may accumulate information on the characteristics of other agents and on potential coalitions and coalitional structures.

We define $\underset{\mathcal{C}}{\mathcal{M}}$ a finite set of agents such that $\underset{\mathcal{C}}{\mathcal{M}} \subseteq \mathcal{M}$,where each member of this set (group of maintenance crew agents) can form a possible coalition $\mathcal{C}$. As stated previously, $m^w \in \mathcal{M}$ are the maintenance crew agents to the water distribution network, and $m^t \in \mathcal{M}$ are the agents associated with the transportation infrastructure and cyber maintenance crew is denoted as $m^l \in \mathcal{M}$. As a result, $\underset{\mathcal{C}}{\mathcal{M}} \subseteq m^w \bigcup m^t \bigcup m^l$.

Let $\underset{\mathcal{C}}{\mathcal{T}}$ be the tasks consisting of failed components (i.e., roads, pipes or traffic lights) which the coalition will work to restore them. To define reward / utility function for each coalition $\underset{\mathcal{C}}{\mathcal{R}}$, we first use Dijkstra shortest path algorithm to determine the distance between agents and failed components, and assign the reward based on proximity among them. In other words, nodes further away from one another will be assigned a smaller reward compared to nodes closer. The goal is to minimize the distance function. We define distance between maintenance crew agents as d_{ij} where i is source agent and j is target agent. We define d_{ik} as the distance between agents and failed component where i is the agent and k is the failed component. w_1 and w_2 are the weight associated for each distance function. It should be note that the coalitions can be formed between and within agents representing water and transportation sectors (e.g., water and road, road and road, road and traffic lights).

$$\mathcal{Z}_1 = \underbrace{w_1 \times \sum_{i=1}^{\mathcal{M}_{\mathcal{C}}} \sum_{j=1}^{\mathcal{M}_{\mathcal{C}}} d_{ij}}_{\text{Between agents}} + \underbrace{w_2 \times \sum_{i=1}^{\mathcal{M}_{\mathcal{C}}} \sum_{k=1}^{\mathcal{T}_{\mathcal{C}}} d_{ik}}_{\text{Between agents and tasks}}, d_{ij}, d_{ik} > 0, i \neq j \tag{3.1}$$

In the next step, we define the second part of the reward function as the deviation between the expected time of task completion, denoted by e_{ik}, for a maintenance crew compared to actual time taken to complete the task, denoted by c_{ik}.

$$\mathcal{Z}_2 = \sum_{i=1}^{\mathcal{M}_{\mathcal{C}}} \sum_{k=1}^{\mathcal{T}_{\mathcal{C}}} |c_{ik} - e_{ik}| \tag{3.2}$$

It should be noted that the actual completion time for each maintenance crew is a function of their skillset, $0 \leq \alpha_i \leq 1$. Larger values of α_i lead to the minimum deviation between expected and actual completion times. We then normalize both objective functions, Z_1 and Z_2, by using a min-max normalization technique as follows:

$$\mathcal{Z} = \frac{\mathcal{Z} - \mathcal{Z}^{min}}{\mathcal{Z}^{max} - \mathcal{Z}^{min}} \tag{3.3}$$

Finally, the total reward function for coalition $\mathcal{C}$ can be defined as the the aggregation of each component with equal weight of 0.5 as follows:

$$Min \ \mathcal{R}_{\mathcal{C}} = 0.5 \times \mathcal{Z}_1 + 0.5 \times \mathcal{Z}_2 \tag{3.4}$$

It should be noted that an agent can receive offers from multiple agents to form a coalition. However, once a coalition is formed, the agent cannot form another coalition until the coalition goal is reached. After the goal of a coalition is fulfilled, the agents can either form another coalition with different agents or act alone and continue to restore components which are not assigned to any coalition at the time. In addition, we assume that coalition formation is only possible between road maintenance agent and pipe maintenance agent, road maintenance agent and traffic light agent, and among road maintenance agents.

Chapter 4: Implementation and Results

To implement our proposed agent-based simulation, we modeled water and road networks in the city of Tampa. Tampa is a coastal city in Florida with nearly 400,000 populations and is prone to different natural hazards such as hurricanes and floods. The simulation model was developed in AnyLogic, a Java-based platform. Fig. 4.1 shows the overlaid simplified water and transportation networks in our simulation model.

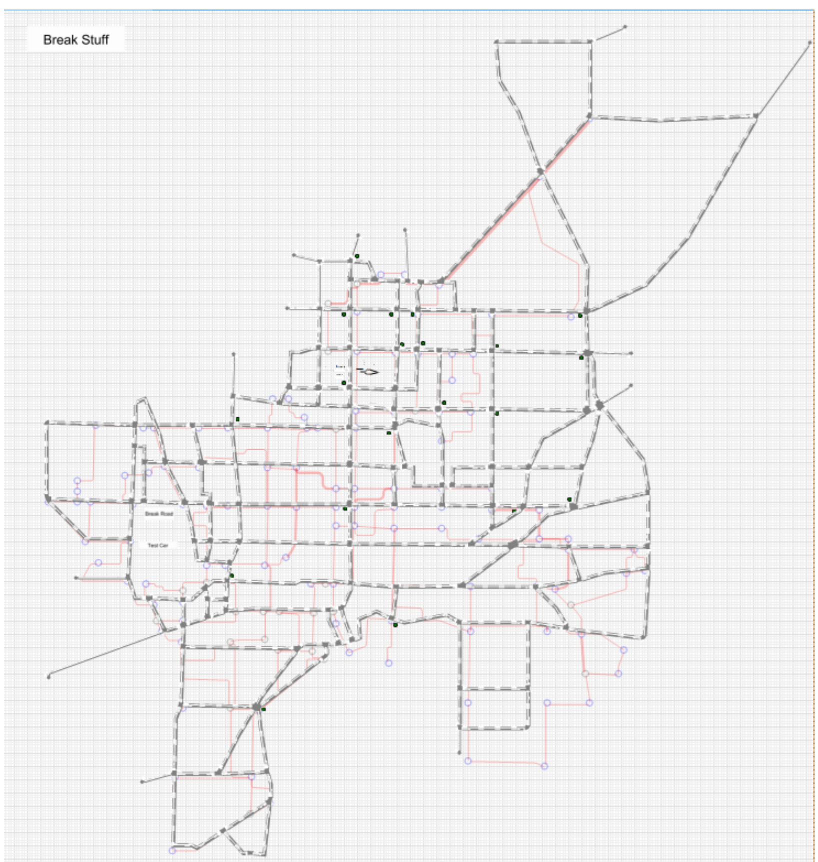

Figure 4.1 Simplified interdependent water and transportation network

4.1 Parameters and Verification

We first allocated two maintenance agents to each department, including water, road and traffic light. The restoration time for each road segment $r \in \mathcal{R}$ by having m maintenance crew teams is defined as τ_r and can be calculated by the following equation:

$$\tau_r = \frac{D_1 + D_2 + D_3 + D_4}{m} \tag{4.1}$$

Where D_1 is the *days to mill asphalt* and can be obtained for a road pavement r being restored (in yd^2) and the production rate of α_a by the following formulation:

$$D_1 = \frac{r}{\alpha_a} \tag{4.2}$$

Likewise, D_2 is the *days to mill base* and can be obtained for a road pavement r being restored (in yd^2) and the production rate of α_b by the following formulation:

$$D_2 = \frac{r}{\alpha_b} \tag{4.3}$$

For estimating the required *days to restore structural course* defined as D_3 for a road pavement r being restored (in yd^2), the production rate of α_{bsc}, and depth of structural course h_{sc}, we use the following formulation:

$$D_3 = \frac{r \times h_{sc}}{\alpha_{sc}} \tag{4.4}$$

However, for D_4 reflecting *days to restore friction course*, a graphical function based on friction course being restored is used, which is defined for a road pavement r being restored (in yd^2), the production rate of α_{fc}, and Spread rate β_{fc}, we use the following formulation:

$$D_4 = \frac{\alpha_{fc} \times r \times \beta_{fc}}{2000} \tag{4.5}$$

The restoration time for each pipe $p \in \mathcal{P}$ with length o_p in feet and having α_w water main installation production rate is defined as τ_p can be calculated by the following equation:

$$\tau_p = o_p \times \alpha_w \tag{4.6}$$

The restoration time for traffic lights is assumed to follow a uniform distribution between 25 and 35 minutes, which is obtained from expert opinions.

We then calibrated the model through a systematic and iterative process to ensure that the output of the simulation framework is reliable. In specific, we adopted various internal and external approaches to verify the data, logic, and computational algorithms in the simulation model. First, we ensured that the simplified water and transportation networks represent the original source in terms of completeness, coherence, and correctness on the infrastructure level. We defined the traffic flow based on the O-D (origin-destination) matrices across the study region for the road network. We also conducted a spatial analysis to assign the most accurate diameter and flow to each aggregated pipe based on actual water network components. We utilized the signal data to imitate the behavior of traffic lights in each phase transformation among different states.

To verify the output of the simulation framework in terms of simulated traffic, we selected a set of 5 roads in the four geographical zones in the study area. In specific, the selected roads are the longest in each segment. We obtained the historical daily traffic information from the Florida Department of Transportation Traffic online web application [1]. This interactive database provides the daily traffic information for all the road sections in Tampa between 2017 and 2021. As the aggregated transportation network is embedded in the agent-based model, we selected the closest actual road in the original network to conduct the comparison. We performed a statistical t-test for each selected road section and provided the statistical analysis output in Table 4.1. The p-values of the test show that the differences between real and simulated traffic for all

[1]https://tdaappsprod.dot.state.fl.us/fto/

segments are statistically insignificant.

Table 4.1 Road traffic verification result

		Real Data		Simulated Data				
Road ID	**Zone**	Mean	Variance	Mean	Variance	**df**	t-**Statistic**	p-**value**
9	1	65600	1781.85	63221.59	3554.525	13	-1.73	0.187
12	1	43400	2459.675	44627.644	8361.787	13	0.43	0.676
105	2	25540	3362.737	25603.465	1816.936	13	0.04	0.97
230	3	25260	2581.279	24455.391	962.274	13	-0.67	0.537
244	4	23500	3917.269	26253.447	1181.960	13	1.54	0.199

4.2 Computational Study

We designed various disruptive scenarios to assess the resilience of interdependent water and transportation in dealing with failures. As summarized in Table 4.2, two main groups of scenarios are defined:

1. **Physical Failures**: In this set of scenarios, we assume that the only source of failure is the functional disruptions in the physical component (e.g., pipes in water and road intersections in the transportation network). We run the simulation framework for 7 days to monitor the performance of the interconnected system in dealing with these incidents.

2. **Cyber-physical Failures**: The second part of scenarios is designed to assess the impact of simultaneous physical failures and cyber-attacks on traffic lights (behave differently than the predefined signalling phases). In these experiments, we mainly focus on the impact of compound failures on the water-transportation network on the improvement of resilience. Similar to physical scenarios, we simulated this class for 7 days to capture the long-term effect of cyber-physical disruptions on the

partial and overall resilience of sub-systems and the system-of-system entity, respectively.

It should be noted that we simulated each disruptive scenario 10 times for each collaboration structure, presented in Chapter 3, to assess the value of coordination strategies on the enhancement of resilience analysis.

Table 4.2 Disruptive scenarios

Failure type	Scenario ID	Water failure	Transportation failure	Cyber failure	Duration
Physical	SC1	5%	5%	x	7 days
	SC2	10%	10%	x	
	SC3	15%	15%	x	
	SC4	20%	20%	x	
	SC5	25%	25%	x	
Cyber-physical	SC11	5%	5%	5%	7 days
	SC12	10%	10%	10%	
	SC13	15%	15%	15%	
	SC14	20%	20%	20%	
	SC15	25%	25%	25%	

4.2.1 Performance Metrics

System Resilience

There are several references in the literature of critical infrastructure including [27], [28], and [29] stating that the functional length of an infrastructure network is an appropriate indicator to capture the resilience toward failures. Consistent with these studies, we use a length-based quantitative measure to capture the resilience concept of the interdependent network to cyber-physical failures. In specific, we assume that the total length of water network is $\mathcal{L}_w$ and the overall operational length of this in step n network is $\mathcal{O}_w^n$. We calculate the resilience of water network in step n of simulation is as follows:

$$\mathcal{R}_w^n = \frac{\mathcal{O}_w^n}{\mathcal{L}_w},\ 0 \leq \mathcal{R}_w^n \leq 1, \forall n \in \mathcal{N}. \tag{4.7}$$

Likewise, we define the overall length of transportation and the functional length in step n as $\mathcal{L}_t$ and $\mathcal{O}_t^n$, respectively. Therefore, the partial resilience of transportation in step n simulation is as follows:

$$\mathcal{R}_t^n = \frac{\mathcal{O}_t^n}{\mathcal{L}_t},\ 0 \leq \mathcal{R}_t^n \leq 1, \forall n \in \mathcal{N}. \tag{4.8}$$

We also defined the resilience of the traffic light network in a similar method. However, since the concept of length is meaningless for traffic lights, we tailored the idea and used the number of operational lights $\mathcal{O}_l^n$ and the total number of lights in the system $\mathcal{L}_l$ to calculate the resilience in step n of simulation as follows:

$$\mathcal{R}_l^n = \frac{\mathcal{O}_l^n}{\mathcal{L}_l},\ 0 \leq \mathcal{R}_l^n \leq 1, \forall n \in \mathcal{N}. \tag{4.9}$$

Now, we can measure the resilience of the interdependent network system $\mathcal{R}_\mathcal{S}$ consisting of s sub-systems in step n of simulation as the average of partial resilience of individual components (given the assumption that all partial systems contribute equally to the resilience metric of overall network) as follows:

$$\mathcal{R}_\mathcal{S}^n = \frac{\sum_{i=1}^{|s|} \mathcal{R}_s^n}{|s|},\ 0 \leq \mathcal{R}_\mathcal{S}^n \leq 1, \forall n \in \mathcal{N}. \tag{4.10}$$

In this equation, $\mathcal{N}$ is the set of simulation steps before the termination condition (simulation duration) is met and $|s|$ is the number of sub-systems contributing to the main system.

Ranked Ordered Resilience Curve

The overall system resilience curves provide valuable information about the restoration trajectory of the interdependent network; however, they fail to reflect how each system responded to disruptions. To bridge this gap, we adopted the rank aggregation idea originally presented in [30] and later refined in [31] to evaluate the accuracy of predictive models in predicting the failure rates of highly vulnerable components in a network. We tailored this idea to capture how decision-makers at the municipality level prioritized the limited budgets and resources to restore the disrupted parts and improve resilience. In this study, we assumed that the network's resilience is directly related to its operational length, meaning that prioritizing the restoration of longer components (pipes and road segments in our case) will expedite the system's recovery to the pre-disaster performance level. Therefore, in the Ranked Ordered Curve, we capture the proportion of the restored length of the network (also an indicator of partial resilience for that network) to the restoration capture.

Assume that the restored length in each restoration epoch i is defined as l^i, the cumulative length of restored network ξ and the cumulative simulation step ω for epoch time $\mathcal{T}$ are calculated as follows:

$$\xi = \sum_{i=1}^{\mathcal{T}} l^i, \;\; \omega = \sum_{i=1}^{\mathcal{T}} i. \tag{4.11}$$

Given that the total disrupted length in the network is $\mathcal{L}$ and the total number of steps in the simulation is $\mathcal{N}$, the coordination of the associated point $\mathcal{P}$ for this epoch of time is calculated as follows:

$$\mathcal{P}_x^t = \frac{\omega}{\mathcal{N}}, \;\; \mathcal{P}_y^t = \frac{\xi}{\mathcal{L}}. \tag{4.12}$$

Where $\mathcal{P}_x^t$ shows the proportional restoration capture and $\mathcal{P}_y^t$ reflects the proportional length capture in the Ranked Ordered resilience curve.

The $AUC = 1$ is the optimal situation where the system could restore all the failed components in one effort, and the curve jumps to the maximum level of length capture for the rest of the simulation time. In contrast, $AUC = 0$ indicates that the network's administrators performed no restorative action following a disruption. Therefore, the value of $0 \leq AUC \leq 1$ in a real-life setting and the higher values of this indicator show that the decision-makers prioritized the recovery of more critical components (e.g., longer pipes and roads that serve more demand points) to accelerate the resilience enhancement. We calculated this performance measure for water and transportation networks for all failure scenarios and communication protocols to comprehensively analyze each infrastructure. We also added a baseline to these figures ($AUC = 0.5$) to reflect a conservative strategy regarding network restoration. In this strategy, the overall length of disrupted components is equally distributed among restoration steps. Therefore, a value of $AUC \geq 0.5$ shows that the recovery plan is designed based on a good prioritization of longer (in our case, vital to enhancing the resilience). On the other hand, as the curve becomes more distant (on the lower triangle), the restoration efficiency deteriorates.

4.2.2 Simulation Output

The resilience curves for all collaboration structures show that the system recovery deteriorates as the magnitude of failure increases inside the interdependent network (see Figures 4.2-4.7).However, we observe that when the collaboration structure is defined by the decentralized coalition formation protocol, the network can recover to the pre-disaster operational level for all simulation instances in the 5% failure scenario (both physical and cyber-physical). In addition, we observe tighter confidence intervals and less variation for the decentralized coalition formation protocol compared to other collaboration structures.

The system behaves differently for the 10% and 15% failure scenarios by continuously improving resilience during 7 days of restoration horizon. However, as the system experienced a more severe impact, the restored service level is lower than the standard level. Under the decentralized coalition formation protocol, the average resilience of the water-transportation system is approximately 0.985 and 0.96 for the 10% and 15% failure scenarios, which is significantly higher compared to other coordination protocols. In the 20% scenario, there is also an improvement in resilience and the average resilience of the water-transportation system is approximately 0.945.

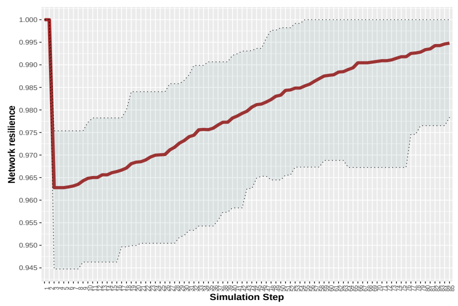

5% failure

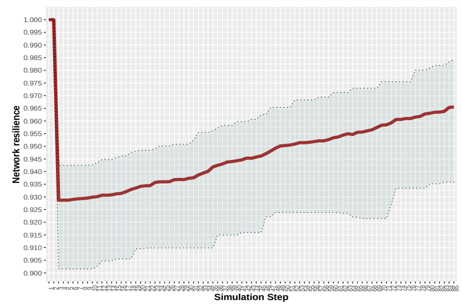

10% failure

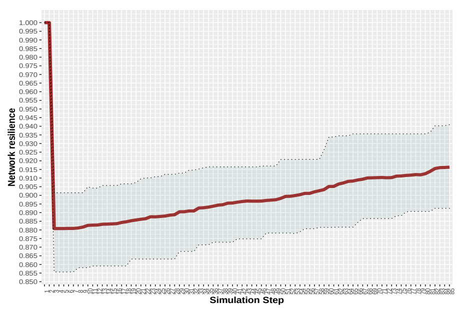

15% failure

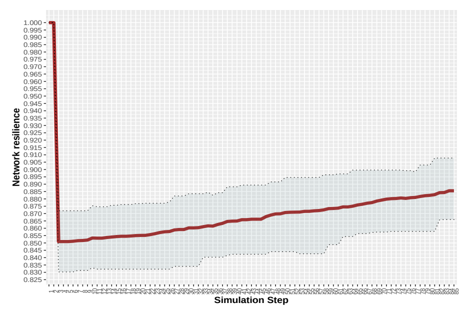

20% failure

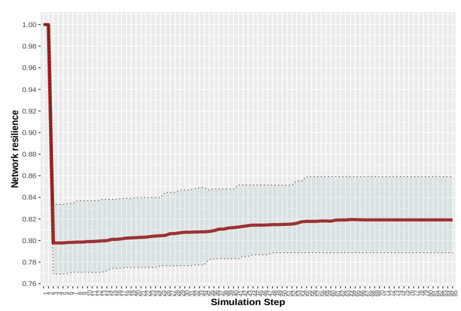

25% failure

Figure 4.2 Network resilience curves for physical failure scenarios and no communication protocol

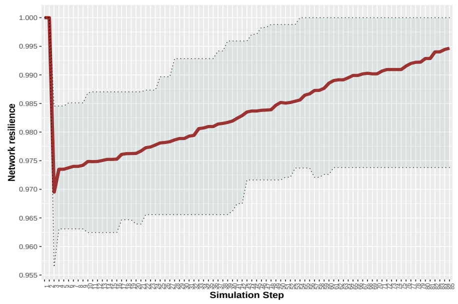

5% failure

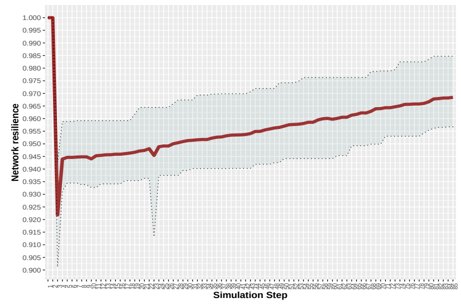

10% failure

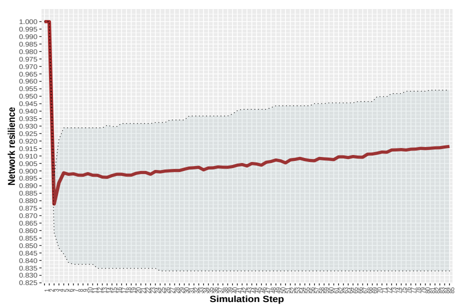

15% failure

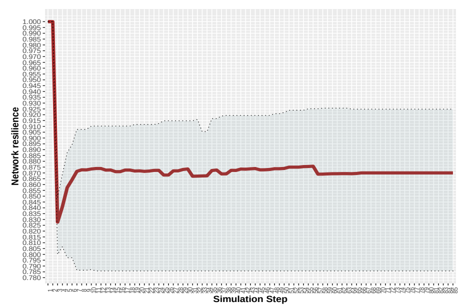

20% failure

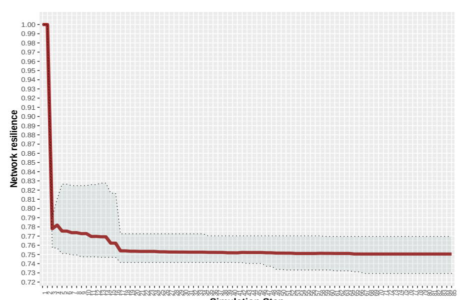

25% failure

Figure 4.3 Network resilience curves for cyber-physical failure scenarios and no communication protocol

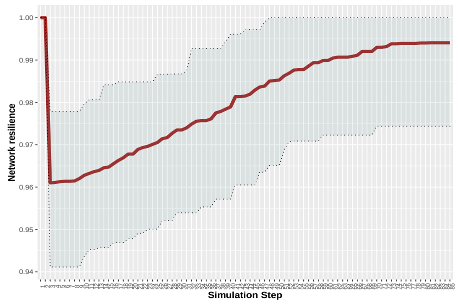

5% failure

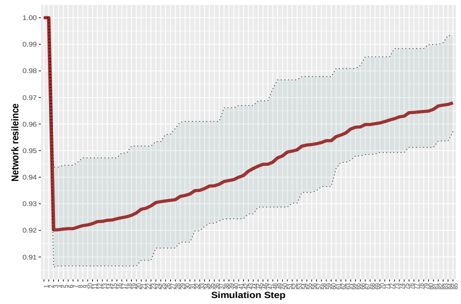

10% failure

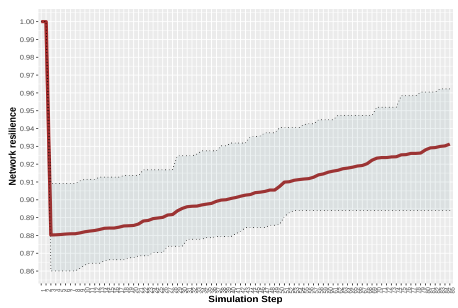

15% failure

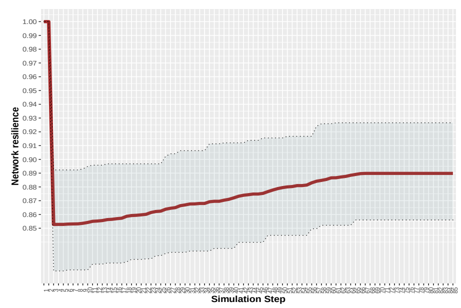

20% failure

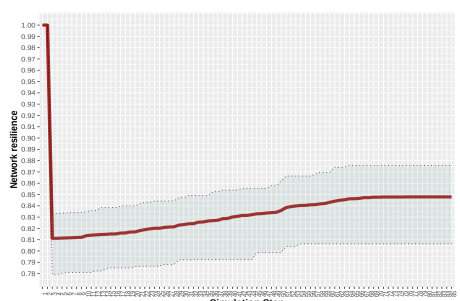

25% failure

Figure 4.4 Network resilience curves for physical failure scenarios and leader-follower coordination protocol

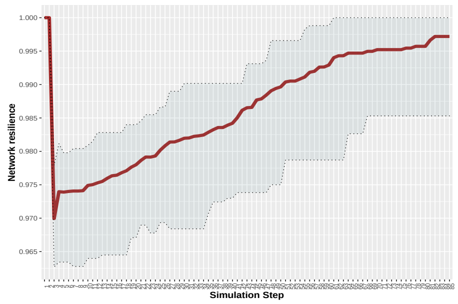

5% failure

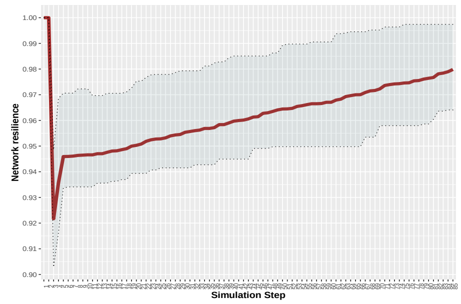

10% failure

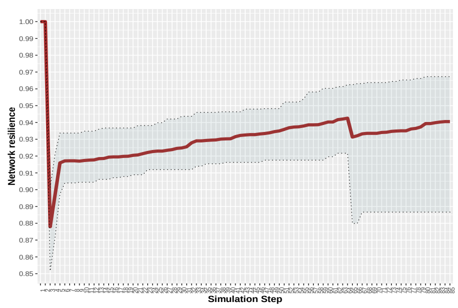

15% failure

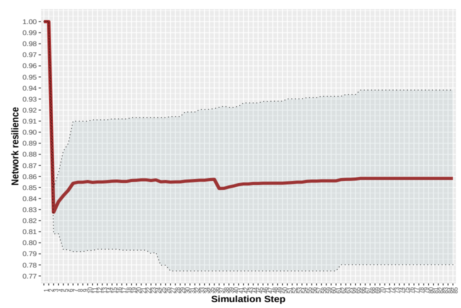

20% failure

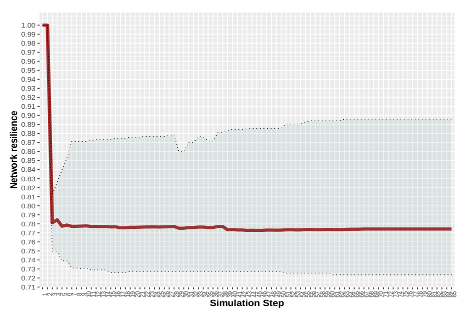

25% failure

Figure 4.5 Network resilience curves for cyber-physical failure scenarios and leader-follower coordination protocol

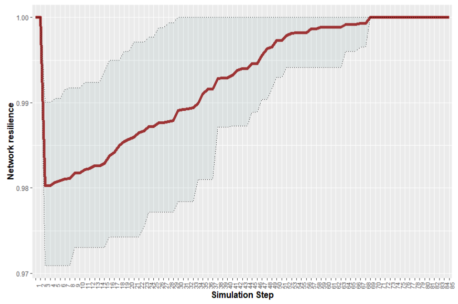

5% failure

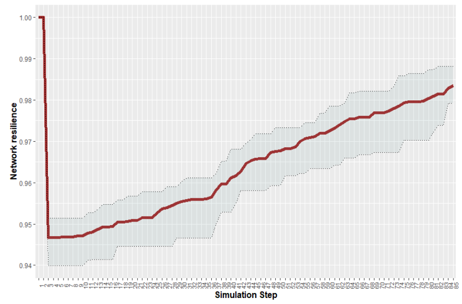

10% failure

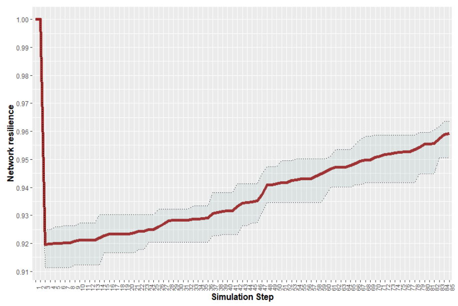

15% failure

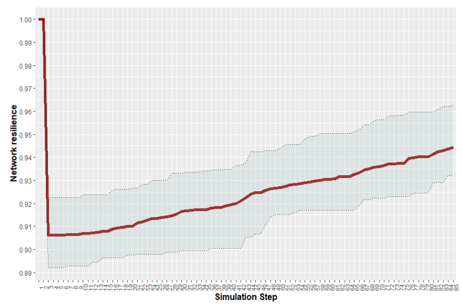

20% failure

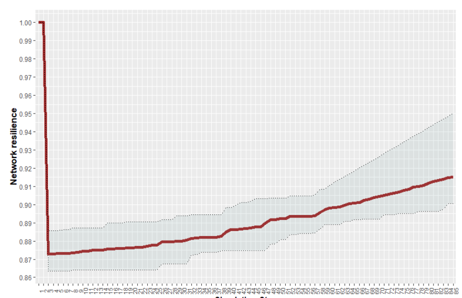

25% failure

Figure 4.6 Network resilience curves for physical failure scenarios and decentralized coalition formation protocol

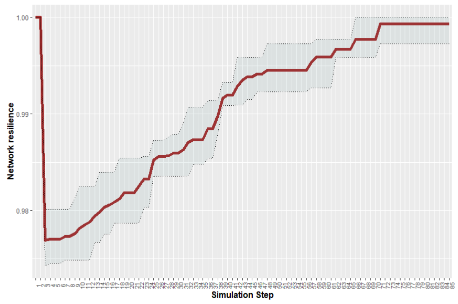

5% failure

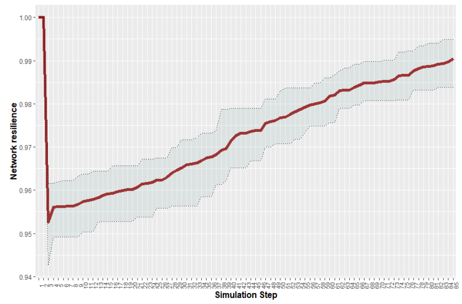

10% failure

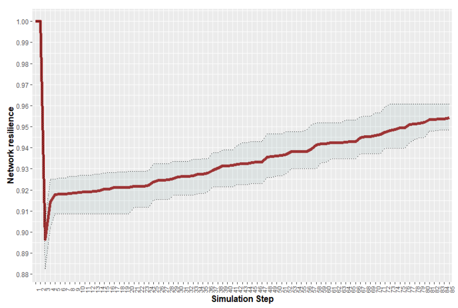

15% failure

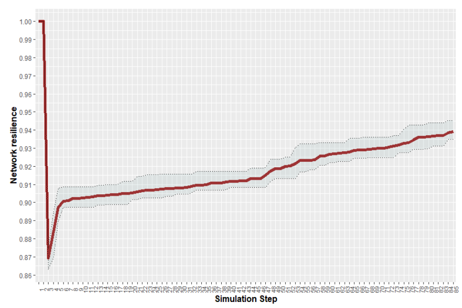

20% failure

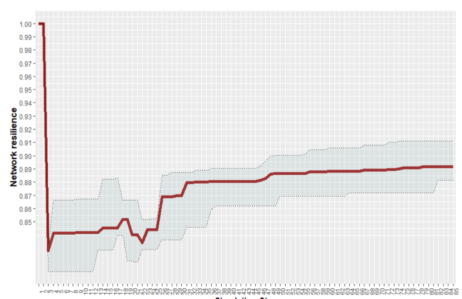

25% failure

Figure 4.7 Network resilience curves for cyber-physical failure scenarios and decentralized coalition formation protocol

Table 4.3 and Figures 4.8-4.13 provide valuable insights into the performance of individual networks and their marginal contribution to the overall resilience improvement. For the physical failure scenarios, both leader-follower and decentralized coalition formation protocols outperform the no communication protocol. In addition, it appears that the AUC metric is higher for the leader-follower coordination protocol, while the difference is more tangible for the lower magnitude of failures. However, as the failures become more significant, the AUC for different protocols does not reflect a notable difference. This observation can be attributed to the limited number of available maintenance crews responsible for the restoration of networks. In other words, the impact of adopting different communication protocols to improve resilience is directly relevant to have more resources to be assigned to disrupted components.

For the cyber-physical failure scenarios, all coordination structures lead to an $AUC \leq 0.5$ for both water and transportation networks. For the 5% and 10% scenarios, the decentralized coalition formation protocols outperforms the no communication protocol. As the magnitude of failures increases, we do not observe significant differences among coordination structures which is the reflective of limited resources for restoring the interdependent networks.Nonetheless, for the 25% scenario, the decentralized coalition formation outperforms both no communication and leader-follower protocols.

Overall, it can be observed that the cyber-physical failures significantly disrupt the performance of infrastructure networks. Physical failures impose financial and social pressure on infrastructure systems through huge restoration costs and lost demand of vulnerable communities. However, the high dependency of modern infrastructure systems on cyber components worsens the situation and indicates the need to strengthen the systems' preparedness to absorb the possible cyber-attacks impacts and expedite recovery. In addition, the resilience improvement of the interconnected network experienced different trajectories. The limited number of maintenance crews in both networks showed that the resources are inadequate to respond to large-scale failures.

The simulation results also demonstrated that both leader-follower and decentralized coalition formation protocols could positively contribute to restoring interdependent networks. We can infer that while in a decentralized decision-making environment, each sub-system administrator is concerned about their partial recovery, the coordination could result in a better overall restoration of the system-of-system.

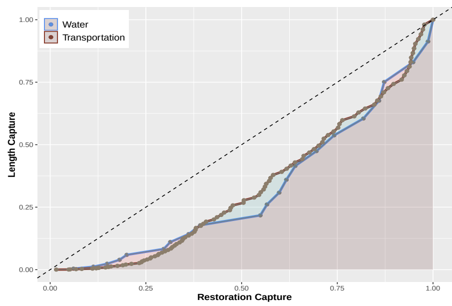

5% failure

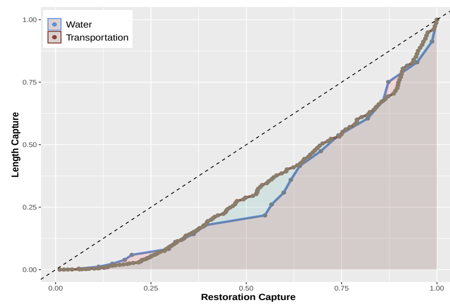

10% failure

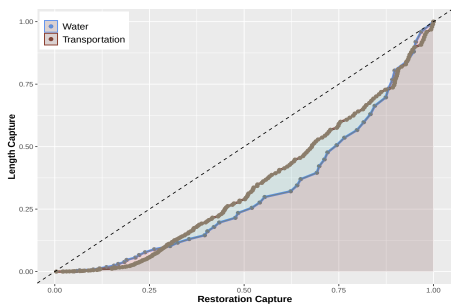

15% failure

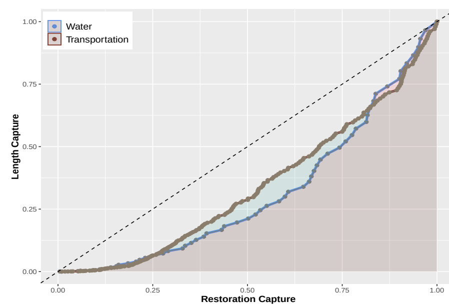

20% failure

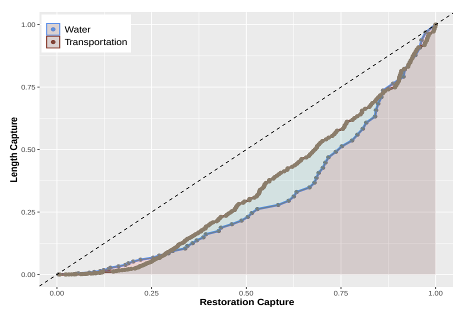

25% failure

Figure 4.8 Ranked Ordered resilience curve for physical failures scenarios and no communication protocol

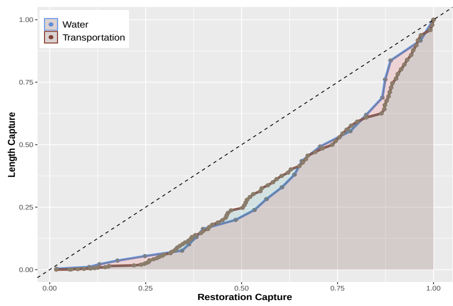

5% failure

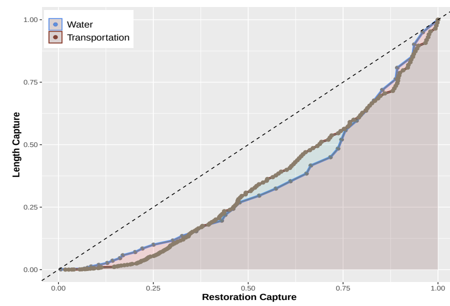

10% failure

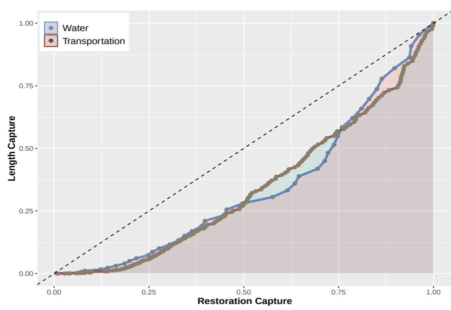

15% failure

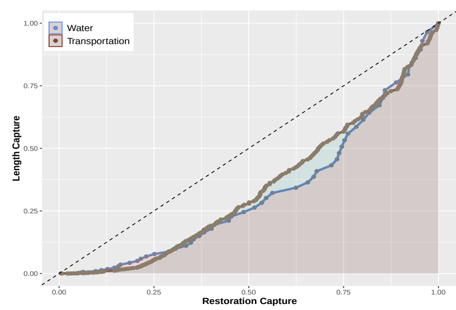

20% failure

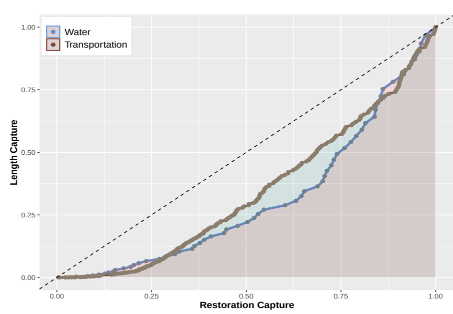

25% failure

Figure 4.9 Ranked Ordered resilience curve for cyber-physical failure scenarios and no communication protocol

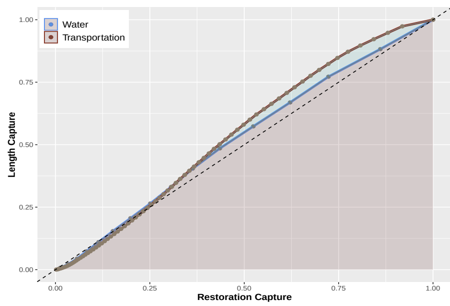

5%failure

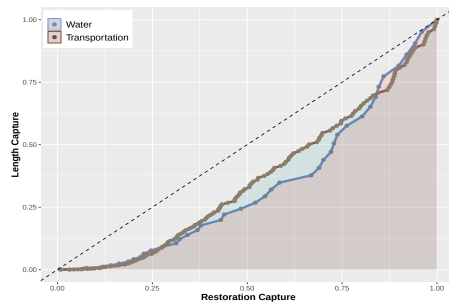

10% failure

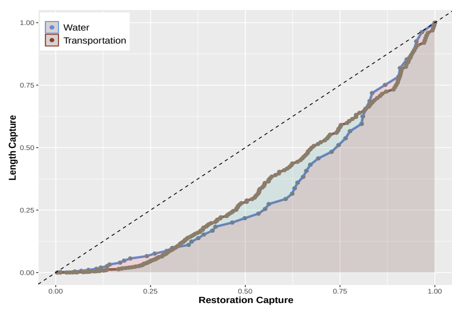

15% failure

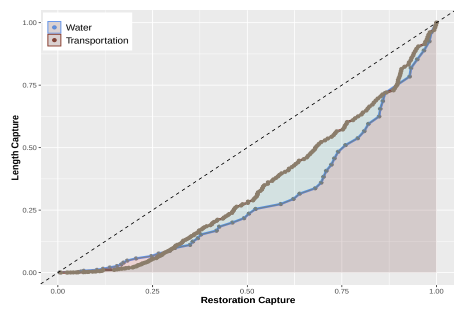

20% failure

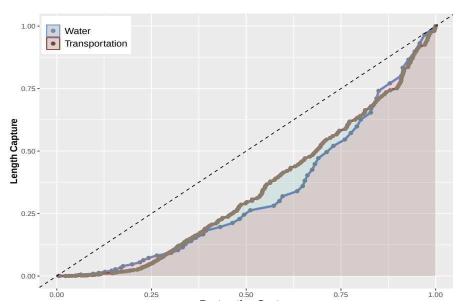

25% failure

Figure 4.10 Ranked Ordered resilience curves for physical failures and leader-follower coordination protocol

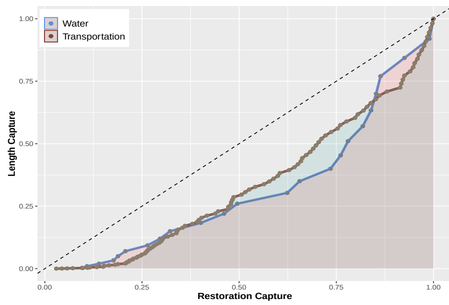

5% failure

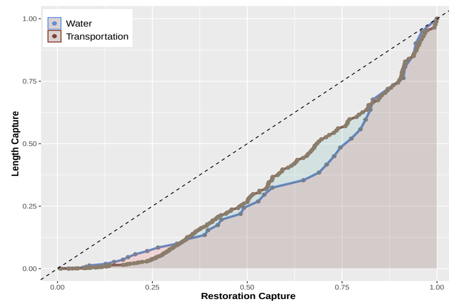

10% failure

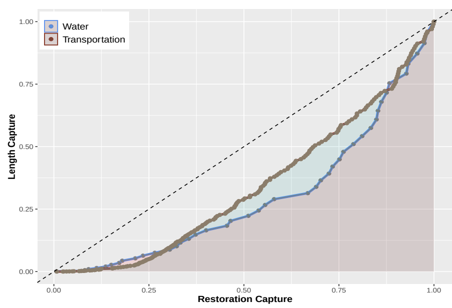

15% failure

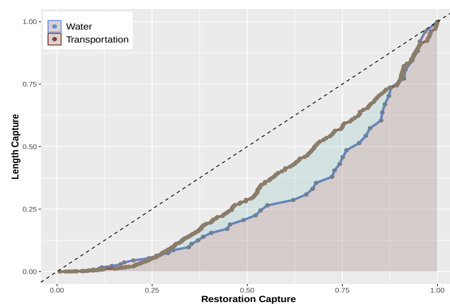

20% failure

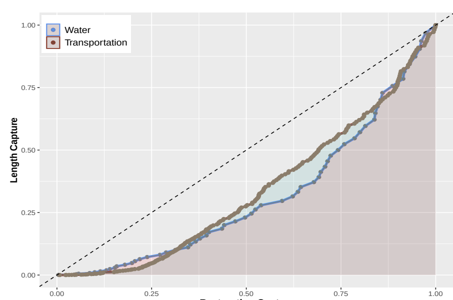

25% failure

Figure 4.11 Ranked Ordered resilience curves for cyber-physical failure scenarios and leader-follower coordination protocol

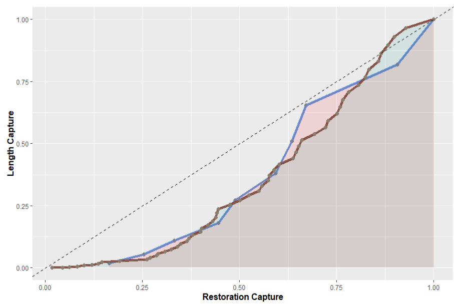

5% failure

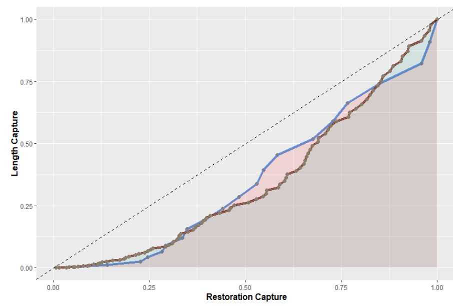

10% failure

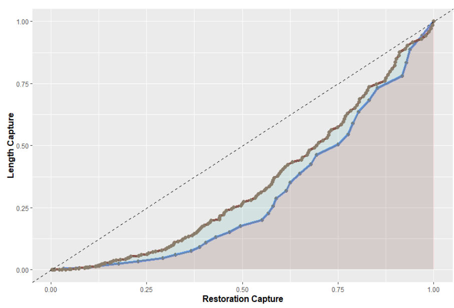

15% failure

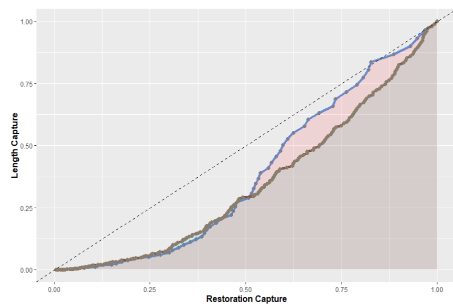

20% failure

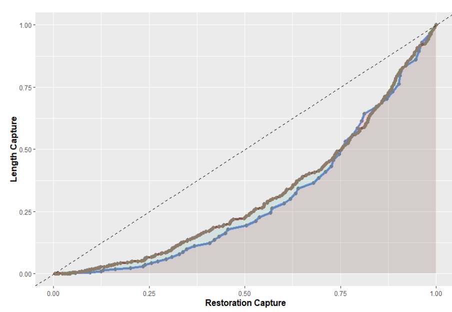

25% failure

Figure 4.12 Ranked Ordered resilience curves for physical failure scenarios and decentralized coalition formation protocol

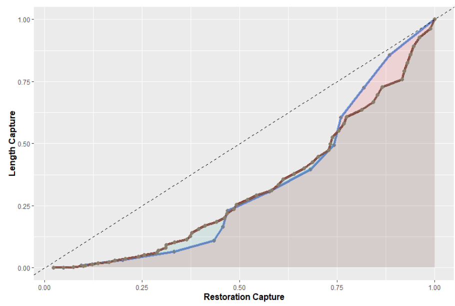

5% failure

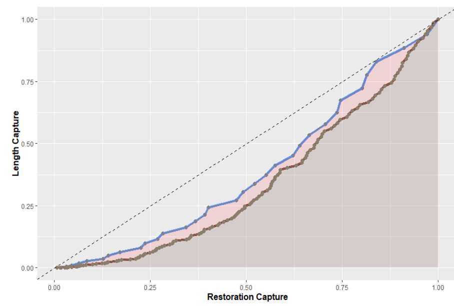

10% failure

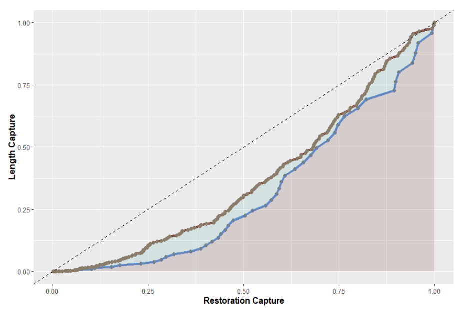

15% failure

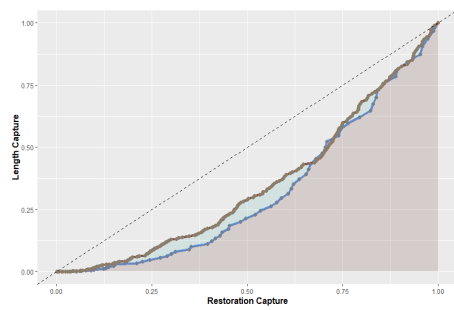

20% failure

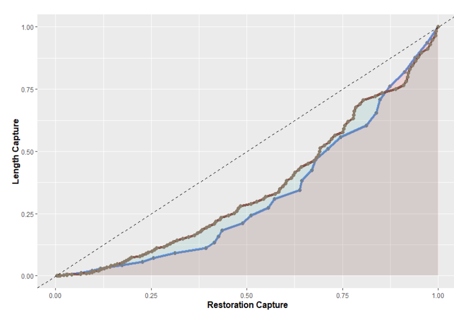

25% failure

Figure 4.13 Ranked Ordered resilience curves for cyber-physical failure scenarios and decentralized coalition formation protocol

Table 4.3 Area under the curve for different Communication Protocols

Failure type	Communication Protocol	Failure Scenario	Water AUC	Transportation AUC
Physical	Leader-follower	5%	0.526	0.548
		10%	0.333	0.359
		15%	0.320	0.340
		20%	0.299	0.341
		25%	0.327	0.345
	No communication	5%	0.315	0.328
		10%	0.316	0.332
		15%	0.315	0.347
		20%	0.312	0.341
		25%	0.310	0.345
	Decentralized coalition formation	5%	0.368	0.362
		10%	0.356	0.346
		15%	0.300	0.346
		20%	0.349	0.386
		25%	0.316	0.295
Cyber-physical	Leader-follower	5%	0.312	0.328
		10%	0.315	0.334
		15%	0.294	0.339
		20%	0.292	0.344
		25%	0.313	0.337
	No communication	5%	0.317	0.314
		10%	0.338	0.340
		15%	0.339	0.338
		20%	0.324	0.341
		25%	0.309	0.342
	Decentralized coalition formation	5%	0.324	0.318
		10%	0.390	0.340
		15%	0.318	0.371
		20%	0.318	0.349
		25%	0.321	0.351

Chapter 5: Conclusions

In this thesis, we designed and implemented an agent-based simulation model to analyze the resilience of interdependent infrastructure networks to cyber-physical failures. The agent-based model could capture the complex and dynamic behaviour of agents during and after disruptive events. The modeling approach allowed us to overcome the common simplifications in mathematical modeling studies of centralized decision-making configuration. The model consisted of a water distribution system and transportation network (physical components) and traffic light network (cyber component). We defined the repair crews as agents who make decisions at each restoration phase based on the information they receive from the operational environment and their peer entities. By comparing simulated traffic data with real traffic data in the case study area, we were able to verify the simulation model and concluded that the difference between real and simulated traffic were statistically insignificant. We then generated multiple groups of failure scenarios, including physical and cyber-physical, to evaluate the system's resilience to disruptive incidents. We defined three different coordination protocols including no communication, leader-follower, and decentralized coalition formation to investigate how the coordination and information exchange among decision-making units can help with a more efficient restoration of infrastructure systems.

We simulated the framework for 7 days and replicated each simulation scenario 10 times. To measure resilience, we defined a length-based index for water and transportation networks and a similar formulation for the cyber network. In addition to the overall resilience curve, we defined a ranked ordered performance criterion to reflect how each sub-system (e.g., individual infrastructure system) can prioritize resilience improvement by restoring the more critical failed elements (longer pipes and roads, for example). The results showed that the interdependent system is more under pressure from compound cyber-physical failures than isolated physical scenarios. In addition, the no-communication protocol, where there is no information sharing between different groups of agents, performed poorly compared to other coordination protocols. With no information sharing, we observed redundancy in resource allocation for interdependent infrastructure. Leader-follower coordination protocol was able to overcome the shortcomings of no communication protocol by introducing information sharing between leaders (water crew) and follower agents (transportation crew). For the compound cyber-physical failures, the decentralized coalition formation protocol, based on a greedy approach, outperforms other coordination protocols for higher magnitudes of failures (i.e., 25%). Overall, we observed tighter confidence intervals and less variation for networks resilience under the decentralized coalition formation protocol.

Restoration process for cyber-physical infrastructure systems is time consuming and a stochastic process. As a result, inefficient resource allocation decisions slow down the network recovery significantly. The simulation model, implemented in this study, could be used for different what-if analyses to assess restoration strategies with respect to different collaboration schemes and magnitudes of failures. It is evident that more information sharing among agents contributes to better coordination and network resilience. However, the cost of information exchange and its impact on computational time is not considered in this study. We used a greedy approach for the coalition formation process which resulted in a fewer coalitions after the first round of coalition formation. Future research could design learning agents which can form coalitions based on their past experience in later stages of the restoration activities.

Bibliography

Bibliography

[1] DHS, "Us department of homeland security, critical infrastructure sectors," 2021, accessed: 2021-03-04. [Online]. Available: https://www.dhs.gov/cisa/critical-infrastructure-sectors

[2] T. R. Shift. The resilience shift critical infrastructure resilience for a safer and better world.

[3] S. Resetar, L. Ecola, R. Liang, D. Adamson, C. Forinash, L. Shoup, B. Leopold, and Z. Zabel, "Guidebook for multi-agency collaboration for sustainability and resilience," 2020.

[4] Fema. (2021) Collaborating to build resilience. [Online]. Available: https://www.fema.gov/case-study/collaborating-build-resilience

[5] NSF. (2018) Better coordination networks to strengthen interdependent infrastructure resilience. [Online]. Available: https://beta.nsf.gov/news/better-coordination-networks-strengthen

[6] P. M. Baidya and W. Sun, "Effective restoration strategies of interdependent power system and communication network," *The Journal of Engineering*, vol. 2017, no. 13, pp. 1760–1764, 2017.

[7] M. Ouyang, "Review on modeling and simulation of interdependent critical infrastructure systems," *Reliability engineering & System safety*, vol. 121, pp. 43–60, 2014.

[8] C. B. N. H. H. J. M. J. W. W. Sharkey, T., "Interdependent network restoration: on the value of information-sharing. european journal of operational research," *European Journal of Operational Research*, vol. 244, p. 309–321, 2015.

[9] A. Esmalian, W. Wang, and A. Mostafavi, "Multi-agent modeling of hazard-household-infrastructure nexus for equitable resilience assessment," *arXiv preprint arXiv:2106.03160*, 2021.

[10] S. Ghaffarian, D. Roy, T. Filatova, and N. Kerle, "Agent-based modelling of post-disaster recovery with remote sensing data," *International Journal of Disaster Risk Reduction*, vol. 60, p. 102285, 2021.

[11] J. D. Farmer and D. Foley, "The economy needs agent-based modelling," *Nature*, vol. 460, no. 7256, pp. 685–686, 2009.

[12] S. Panzieri, R. Setola, and G. Ulivi, "An approach to model complex interdependent infrastructures," *IFAC Proceedings Volumes*, vol. 38, no. 1, pp. 404–409, 2005, 16th IFAC World Congress. [Online]. Available: https://www.sciencedirect.com/science/article/pii/S1474667016360803

[13] L.A.Bollinger and G.P.J.Dijkema, "Enhancing infrastructure resilience under conditions of incomplete knowledge of interdependencies," *International Symposium for Next Generation Infrastructure Conference Proceedings*, pp. 9–14, 2015.

[14] S. Sukhbaatar, a. szlam, and R. Fergus, "Learning multiagent communication with backpropagation," in *Advances in Neural Information Processing Systems*, D. Lee, M. Sugiyama, U. Luxburg, I. Guyon, and R. Garnett, Eds., vol. 29. Curran Associates, Inc., 2016. [Online]. Available: https://proceedings.neurips.cc/paper/2016/file/55b1927fdafef39c48e5b73b5d61ea60-Paper.pdf

[15] G. Pumpuni-Lenss, T. Blackburn, and A. Garstenauer, "Resilience in complex systems: An agent-based approach," *Systems Engineering*, vol. 20, no. 2, pp. 158–172, 2017. [Online]. Available: https://incose.onlinelibrary.wiley.com/doi/abs/10.1002/sys.21387

[16] J. Fang, S. El-Tawil, and B. Aguirre, "Leader–follower model for agent based simulation of social collective behavior during egress," *Safety Science*, vol. 83, pp. 40–47, 2016. [Online]. Available: https://www.sciencedirect.com/science/article/pii/S0925753515003136

[17] P. S. Rajulapati, N. Nukavarapu, and S. Durbha, "Multi-agent deep reinforcement learning based interdependent critical infrastructure simulation model for situational awareness during a flood event," in *IGARSS 2020 - 2020 IEEE International Geoscience and Remote Sensing Symposium*, 2020, pp. 6890–6893.

[18] N. Saldi, "A topology for team policies and existence of optimal team policies in stochastic team theory," *IEEE Transactions on Automatic Control*, vol. 65, no. 1, pp. 310–317, 2019.

[19] A. Mahajan, N. C. Martins, M. C. Rotkowitz, and S. Yüksel, "Information structures in optimal decentralized control," in *2012 IEEE 51st IEEE Conference on Decision and Control (CDC)*, 2012, pp. 1291–1306.

[20] A. Nayyar, A. Mahajan, and D. Teneketzis, "Optimal control strategies in delayed sharing information structures," *IEEE Transactions on Automatic Control*, vol. 56, no. 7, pp. 1606–1620, 2011.

[21] B. Chen, M. Xu, Z. Liu, L. Li, and D. Zhao, "Delay-aware multi-agent reinforcement learning for cooperative and competitive environments," 2020. [Online]. Available: https://arxiv.org/abs/2005.05441

[22] P. F. Faye, S. Aknine, M. Sene, and O. Shehory, "Dynamic coalitions formation in dynamic uncertain environments," in *2015 IEEE/WIC/ACM International Conference on Web Intelligence and Intelligent Agent Technology (WI-IAT)*, vol. 2, 2015, pp. 273–276.

[23] D. Ahmadoun, E. Bonzon, C. Buron, P. Moraitis, P. Savéant, and O. Shehory, "Decentralized coalition structure formation for interdependent tasks allocation," in *2021 IEEE 33rd International Conference on Tools with Artificial Intelligence (ICTAI)*, 2021, pp. 73–80.

[24] C. Verçosa Pérez Barrios de Souza and F. Enembreck, "Evaluating the impact of reputation-based agents in social coalition formation," in *2016 5th Brazilian Conference on Intelligent Systems (BRACIS)*, 2016, pp. 211–216.

[25] S. Ricker and H. Marchand, "Finding the weakest link(s): Coalition games for decentralized discrete-event control," in *2016 IEEE 55th Conference on Decision and Control (CDC)*, 2016, pp. 3915–3922.

[26] G. Bel, T. Brown, and R. C. Marques, "Public–private partnerships: Infrastructure, transportation and local services," *Local Government Studies*, vol. 39, no. 3, pp. 303–311, 2013. [Online]. Available: https://doi.org/10.1080/03003930.2013.775125

[27] J. Ash and D. Newth, "Optimizing complex networks for resilience against cascading failure," *Physica a: statistical mechanics and its applications*, vol. 380, pp. 673–683, 2007.

[28] D. Henry and J. E. Ramirez-Marquez, "Generic metrics and quantitative approaches for system resilience as a function of time," *Reliability Engineering & System Safety*, vol. 99, pp. 114–122, 2012.

[29] C. Poulin and M. B. Kane, "Infrastructure resilience curves: Performance measures and summary metrics," *Reliability Engineering & System Safety*, vol. 216, p. 107926, 2021.

[30] G. B. Choi, J. W. Kim, J. C. Suh, K. H. Jang, and J. M. Lee, "A prioritization method for replacement of water mains using rank aggregation," *Korean Journal of Chemical Engineering*, vol. 34, no. 10, pp. 2584–2590, 2017.

[31] T. Y.-J. Chen and S. D. Guikema, "Prediction of water main failures with the spatial clustering of breaks," *Reliability Engineering & System Safety*, vol. 203, p. 107108, 2020.

Curriculum Vitae

Mark Herman Dsouza graduated from Mumbai University India in 2019 with a degree in Bachelor of Science in Computer Engineering . He worked as a graduate research assistant under Dr. Shima Mohebbi for a research project. He has 1+ year of experience in JavaScript,Java, Django (Python), SQL, HTML and CSS.